# In situ detection of live-to-dead bacteria ratio after inactivation by means of synchronous fluorescence and PCA

Runze Li[a], Umang Goswami[a], Maria King[b], Jie Chen[c], Thomas C. Cesario[d], and Peter M. Rentzepis[a,1]

[a]Department of Electrical and Computer Engineering, Texas A&M University, College Station, TX 77843; [b]Department of Biological and Agricultural Engineering, Texas A&M University, College Station, TX 77843; [c]Center for Ultrafast Science and Technology, Key Laboratory for Laser Plasmas (Ministry of Education), School of Physics and Astronomy, Collaborative Innovation Center of Inertial Fusion Sciences and Applications (CICIFSA), Shanghai Jiao Tong University, Shanghai 200240, China; and [d]School of Medicine, University of California, Irvine, CA 92697

Contributed by Peter M. Rentzepis, November 16, 2017 (sent for review September 27, 2017; reviewed by Sadik C. Esener and Ting Guo)

**The determination of live and dead bacteria is of considerable significance for preventing health care-associated infection in hospitals, field clinics, and other areas. In this study, the viable (live) and nonviable (dead) bacteria in a sample were determined by means of their fluorescence spectra and principal component analysis (PCA). Data obtained in this study show that it is possible to identify bacteria strains and determine the live/dead ratio after UV light inactivation and antibiotic treatment, in situ, within minutes. In addition, synchronous fluorescence scans enable the identification of bacterial components such as tryptophan, tyrosine, and DNA. Compared with the time-consuming plating and culturing methods, this study renders a means for rapid detection and determination of live and dead bacteria.**

bacteria inactivation | fluorescence spectroscopy | PCA

The determination of live and dead bacteria is of considerable significance in preventing health care-associated infection (HAI) in hospitals, field clinics, and other pathogen-containing areas. HAI is one of the top 10 causes of death in the United States (1) and up to 10% of hospital patients may develop HAI, which adds $5.5 billion extra per year for patient treatment, as estimated by the National Center for Disease Control and Prevention (CDC). These infections transmitted in the hospital environments are especially important because they often are caused by antibiotic-resistant organisms such as methicillin-resistant *Staphylococcus aureus*, vancomycin-resistant *Enterococcus faecium*, *Pseudomonas aeruginosa*, and *Acinetobacter spp* (2). Hospitals cannot continuously search for contamination by these organisms because the monitoring of pathogenic bacteria presented in the environments is a time-consuming process that requires culturing such organisms. Therefore, a rather strong need exists for new surveillance methods that can detect microbial contamination before it causes HAI and continuously monitor for the presence of these bacterial strains and similar populations that cause infections. Likewise, a method to detect immediately bacteria found in wounds, particularly those occurring in remote areas, where neither time nor resources are available to adequately diagnose infection, and to determine if the bacteria were living or dead, would be very useful in initiating early appropriate therapy. In addition, illnesses caused by food-borne bacteria are a global concern that demands rapid detection of pathogens present in food to prevent epidemics of gastrointestinal disease. Early detection of these organisms and knowledge of their viability would be extremely beneficial in preventing outbreaks.

Furthermore, the rapid determination of the evolution of live-to-dead bacteria ratio over time may also be a critical means to determine antibiotic efficacy in treating a specific organism. The CDC has recently estimated that there are 2 million infections and 23,000 deaths a year caused by antibiotic-resistant organisms (3). These resistant organisms commonly found in health care facilities (4, 5) can be resistant to multiple drugs (6–9) and associated with higher mortality rates (10). The need to accurately select the correct antibiotic therapy in this era has been made more acute because of the misuse of currently available antibiotics by inappropriate applications (11) and the fact that new antibiotic development has slowed (11, 12). However, patients currently being treated for an infection typically undergo a rather time-consuming process, which includes specimen collection, empiric initial antibiotic selection, and then waiting while the laboratory processes the specimen, cultures the organism, and completes antibiotic sensitivity testing (13). This traditional process can take a number of days in an era where timely (14) and effective treatment of severe infections can be lifesaving (15). Any method which would accelerate the assessment of antibiotic efficacy could permit essential changes in patient management before the septic process evolves to an irreversible state. Overall, the ability to determine rapidly antibiotic sensitivity and effectiveness is increasingly important as antibiotic resistance becomes a major threat.

Several methods have been proposed for the rapid identification of bacteria, including Raman and fluorescence spectroscopy (16). Three different genera of bacteria: *Escherichia*, *Salmonella*, and *Campylobacter* (all can cause gastrointestinal infections), have been also identified by means of synchronous fluorescence coupled with principal component analysis (PCA) (17). *Lactobacillus* and *Saccharomyces* have been characterized using autofluorescence (18). It may also be possible to classify bacteria strains by excitation at wavelengths that are different for each strain studied. For example, the most appropriate

## Significance

**The in situ and rapid detection of live and dead bacteria is crucial for preventing health care-associated infection in hospitals, field clinics, and other areas such as monitoring wound healings. Traditionally, determining the number of pathogenic organism involves specimen collection, appropriate culture on agar plates within laboratory environments, and counting the colony-forming units. These are very time-consuming procedures and could therefore increase the risk of infection or even death. In this paper, we demonstrate that the live/dead bacteria ratio after UV radiation and antibiotic treatment may be obtained easily, through a handheld spectrophotometer integrated with principal component analysis. Such procedures may provide a new way for the rapid detection and classification of live and dead bacteria in situ within minutes.**

Author contributions: R.L., J.C., T.C.C., and P.M.R. designed research; R.L., U.G., and J.C. performed research; M.K. and J.C. contributed new reagents/analytic tools; J.C., T.C.C., and P.M.R. analyzed data; and R.L., U.G., J.C., and P.M.R. wrote the paper.

Reviewers: S.C.E., University of California, San Diego; and T.G., University of California, Davis.

The authors declare no conflict of interest.



[1]To whom correspondence should be addressed. Email: prentzepis@tamu.edu.

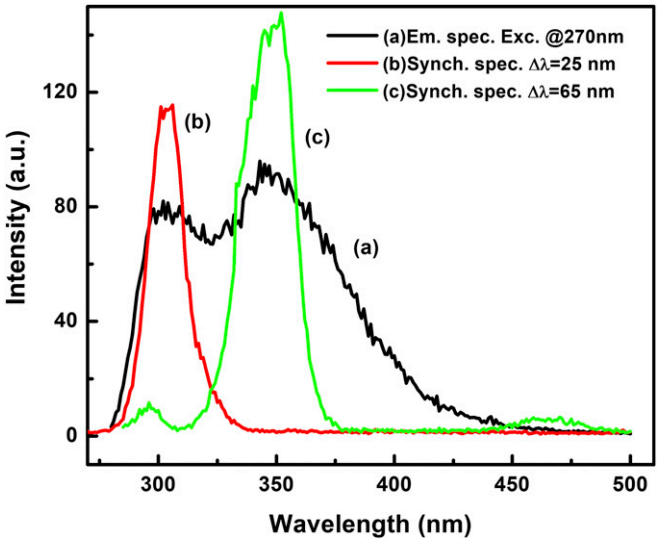


**Fig. 1.** (*a*) Conventional fluorescence spectrum of a tryptophan and tyrosine mixture in saline excited with 270-nm light. (*b*) The synchronous spectra of the same mixture scanned at $\Delta\lambda = 25$ nm show the tyrosine band with a maximum at 310 nm. (*c*) The synchronous spectra of the same mixture scanned at $\Delta\lambda = 65$ nm shows the tryptophan band with a maximum at 350 nm.

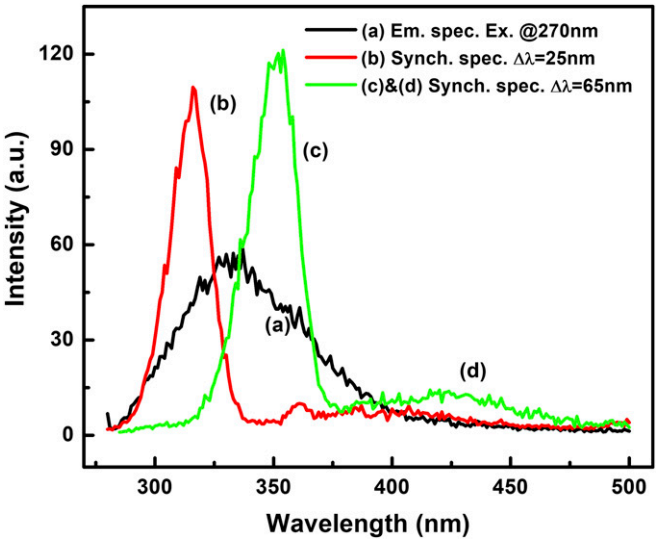


**Fig. 2.** (*a*) Fluorescence spectrum of *Bacillus* at 270-nm excitation wavelength. (*b*) *Bacillus* synchronous spectra scanned at $\Delta\lambda = 25$ nm show the tyrosine band at 310 nm. (*c*) *Bacillus* synchronous spectra scanned at $\Delta\lambda = 65$ nm show the tryptophan band at 350 nm and (*d*) the broad (410~470 nm) low-intensity DNA band.

excitation wavelengths for *Escherichia coli* were found to be 410 and 430 nm, while for bacteria found in meat the best excitation wavelength was found to be 250 nm (19). Therefore, it is possible that those methods could provide an essential answer long before the more traditional method has been completed by reporting a decreased ratio of live-to-dead bacteria.

However, the devices used in previous studies are generally not portable and prolonged operations may be required before obtaining the results. The proper fluorescence recording device should be able to detect and identify in situ within a very short period of time for pathogens in clinics and remote areas and preferably be able to determine the ratio of live over dead bacteria at any time during treatment or after an inactivation process. This information will allow physicians to determine timely, more accurate treatment of infected patients. In this study, we present the design of a handheld fluorescence spectrometer, which coupled with PCA, demonstrates capability of in situ measuring live/dead bacteria ratio. This study renders a means for the rapid detection and classification of live and dead bacteria in situ within a few minutes.

## Experimental

**Synchronous Fluorescence.** Synchronous fluorescence is often chosen as the method for bacteria and mixture components identification because it provides a means for selecting the most appropriate excitation ($\lambda_{exc}$) and emission ($\lambda_{em}$) wavelengths for their detection (20). In conventional fluorescence, the intensity of the emission spectrum depends on the excitation wavelength even though the general spectral features remain the same. However, in the synchronous fluorescence, the intensity $I_s$ is a function of the intensity distribution $E$ of both excitation and emission spectra:

$$I_s = kclE_{exc}(\lambda - \Delta\lambda)E_{em}(\lambda),$$

where $k$ is a sample-dependent constant, $c$ is the concentration of the fluorophore in the sample, and $l$ is the optical beam path length.

While scanning the excitation and emission wavelengths simultaneously, the synchronous technique keeps a constant wavelength offset $\Delta\lambda = \lambda_{em} - \lambda_{exc}$, as shown in the above equation. By properly selecting $\Delta\lambda$, usually matching the difference between the absorption and fluorescence band maxima of the fluorophore of interest, the synchronous method could result in simplified fluorescence spectra with sharper peaks and narrow profiles compared with the conventional method. A rather typical illustration of the conventional and synchronous techniques relevant to bacteria-fluorescing components, tryptophan (Trp) and tyrosine (Tyr), is shown in Fig. 1. The normal fluorescence spectrum of a Trp and Tyr mixture in saline excited with 270 nm is depicted in Fig. 1*A*, which is composed of a

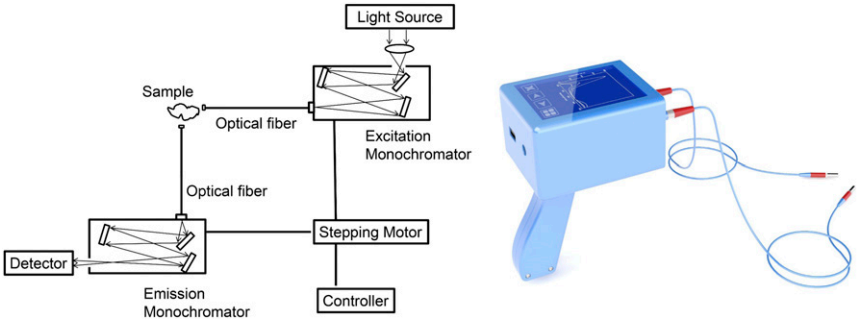


**Fig. 3.** (*Left*) Handheld spectrometer schematic. (*Right*) Conceptual design of the handheld spectrometer appearance with two optical fibers attached to the excitation and emission monochromators. When the two monochromators are coupled together, it allows for the recording of synchronous spectra at a preselected wavelength interval $\Delta\lambda$.

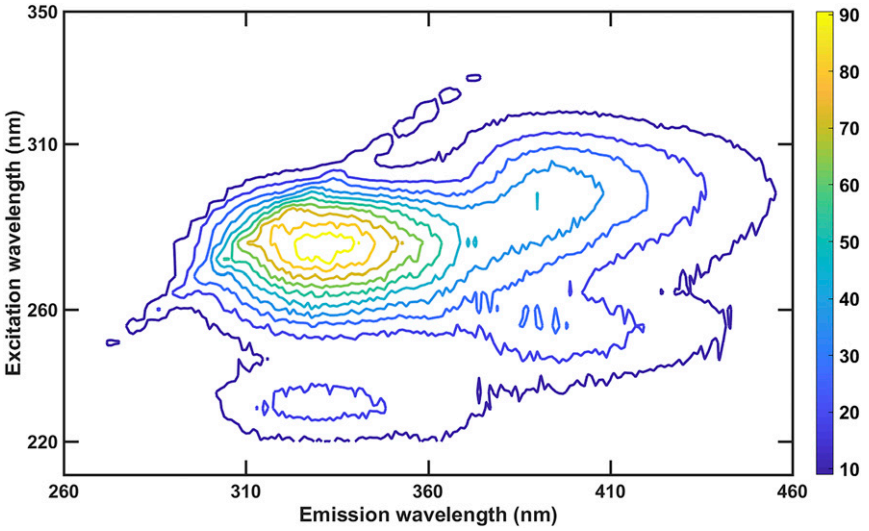


**Fig. 4.** EEM contour of *Bacillus*.

rather structureless broad band that covers the region between 280 and 500 nm, with weak and broad maxima at 300 and 350 nm. Using the synchronous method, the fluorescence spectra of the same amino acids in saline solution show the clearly separated and narrow fluorescence bands of Tyr and Trp with intensity maxima at 310 nm in Fig. 1*B* and 350 nm in Fig. 1*C*, respectively. This emission band separation is due to the fact that $E_{em}(\lambda)$ and $E_{exc}(\lambda)$ are functions limited to different wavelength ranges. Therefore, the corresponding synchronous spectrum, which is a product of $E_{em}(\lambda)$ and $E_{exc}(\lambda)$, exhibits narrow spectral bandwidths, as the Trp and Tyr synchronous fluorescence spectra displayed in Fig. 1 *B* and *C*, respectively, show.

It is rather important to point out that in the conventional fluorescence, which uses a fixed $\lambda_{exc}$, one will increase the emission intensity of all bands simultaneously, but not selectively. In contrast, using the synchronous scan one can selectively increase a particular band by choosing the appropriate $\Delta\lambda$. A pertinent example is shown in Fig. 2, where the emission spectra of tryptophan and tyrosine in *Bacillus* are distinctly displayed. Fig. 2*A* shows the emission spectrum of *Bacillus* excited with 270 nm. Fig. 2*B* depicts the synchronous spectrum of *Bacillus* scanned at $\Delta\lambda = 25$ nm whereupon the tyrosine band at 310 nm is prominent, while Fig. 2*C* was obtained at $\Delta\lambda =$ 65 nm, where the tryptophan band with a maximum at 350 nm is clearly evident. The procedure followed for the identification of the bacteria strains was based on the fluorescing components spectra. For most bacteria, tryptophan is the most intensely fluorescing pigment, followed by tyrosine and the broad, very weakly fluorescing DNA. In this study, we have recorded the changes in fluorescence spectra and intensities of the bacteria and the individual components before and after UV irradiation to determine the mechanism of bacterial inactivation and, in addition, to determine the ratio of live/dead bacteria as a function of radiation dose. To further apply the technique in situ, we have also designed a handheld synchronous spectrometer capable of recording normal and synchronous fluorescence spectra.

**Handheld Spectrometer.** This instrument has been described in detail elsewhere (21). In brief, the handheld synchronous fluorescence spectrometer device, shown in Fig. 3, is composed of three major components: (*i*) two monochromators that are coupled together, (*ii*) two fiber-optic systems, and (*iii*) a two-dimensional charge-coupled device (CCD) detector. The two monochromators, which are used to excite and record the normal and synchronous fluorescence spectra, can scan individually or be coupled together for recording simultaneously, synchronous fluorescence spectra at a preselected wavelength interval $\Delta\lambda$. The first fiber-optics system is used to transmit the excitation light from the excitation monochromator to a sample. The emitted fluorescence from the bacteria sample is collected by the second optical fiber system and focused onto the slit of the fluorescence monochromator and recorded by the CCD, which is coupled to a laptop computer for data processing and PCA.

**Sample Preparation.** *Escherichia coli* (*E. coli*) were obtained from the Bacteriological Epidemiology and Antimicrobial Resistance unit, USDA-ARS. They were cultured in Luria Bertani broth and incubated for 24 h at 37 °C. The bacteria were pelleted and washed with saline twice and then diluted in saline solution before recording their absorption and emission spectra. *Bacillus* bacteria spores were purchased from Sigma-Aldrich. The spores were germinated, incubated for 1 h at room temperature, and suspended in saline before use. The concentration of bacteria used in our experiments varied from $10^5$ to $10^7$ cell per milliliter *E. coli* is a Gram-negative, facultative anaerobe, rod-shaped bacterium that is found in the lower intestine. Many of these *E. coli* strains are harmless, but certain strains are associated with urinary tract or gastrointestinal disease (22, 23). Some *E. coli* bacteria have served as the host for research in recombinant DNA and under favorable

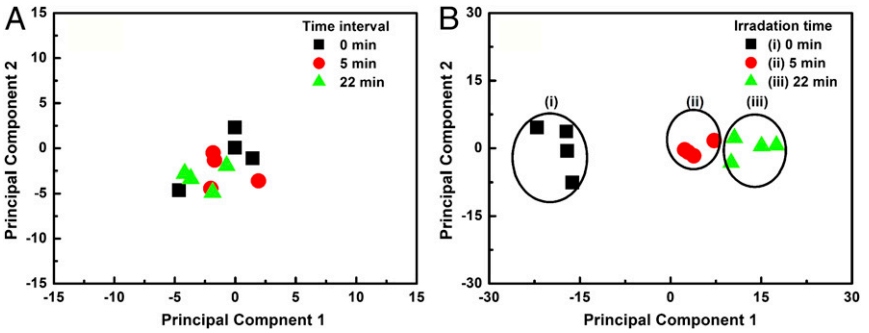


**Fig. 5.** (*A*) PCA of nonirradiated (control) *Bacillus* bacteria. (*B*) PCA of irradiated *Bacillus* bacteria. (*i*), (*ii*), and (*iii*) represented the data that were recorded after 0, 5, and 22 min of UV irradiation, respectively.

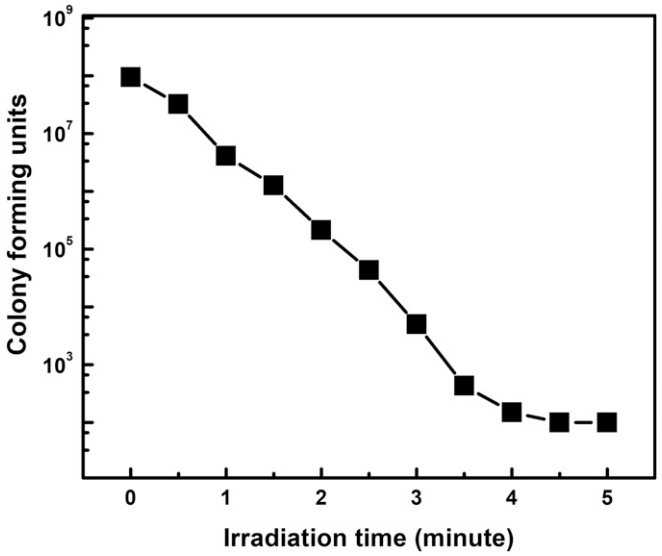


**Fig. 6.** Decreasing of the *E. coli* bacterial population as a function of UV irradiation time. The UV (230~280 nm) irradiation intensity is 5.5 mW/cm$^2$.

conditions, *E. coli* may require only 20 min to reproduce at room temperature. *Bacillus* are Gram-positive genus, rod-shaped bacteria and a member of the phylum Firmicutes, which are ubiquitous in nature. *Bacillus* includes both free-living (nonparasitic) and parasitic pathogenic species (24). These bacteria can produce oval endospores that are not true "spores," but to which the bacteria can reduce themselves and remain in a dormant state for very long periods of time. *Bacillus* can produce copious amounts of enzymes which are used by different industries; however, other species of *Bacillus* are important pathogens, causing anthrax and food poisoning.

**Spectra.** In addition to using the handheld synchronous fluorescence spectrometer, the absorption spectra and fluorescence spectra in the range of 200 and 800 nm were also recorded by a Shimadzu UV-160 spectrometer and a Shimadzu RF-5301PC spectrofluorimeter, respectively. The samples were measured in high-quality quartz cells with a 1-cm optical path length. Measurements were made either at the temperature maintained with ice to reduce bacteria reproduction, or at room temperature to simulate environmental conditions. For synchronous spectra, the excitation was measured between 220 and 490 nm. The $\Delta\lambda$ varied from 10 to 125 nm and the fluorescence spectra were recorded from 230 to 700 nm at 1-nm intervals. Twenty-four spectra were recorded per sample. The optimum excitation–emission wavelengths were decided by the synchronous methods based on the scanning interval $\Delta\lambda$ determined by both excitation–emission matrix (EEM) contours and the wavelength difference in absorption and emission peaks. To that effect Fig. 4 shows that the best $\Delta\lambda$ for the synchronous fluorescence of *Bacillus* is 65 nm, while scanning at this $\Delta\lambda$ the saline solution did not display any detectible fluorescence.

## Results and Discussion

**PCA.** The recorded fluorescence spectra were used in conjunction with PCA, which made it possible to identify the bacteria strain and in addition, determine the ratio of live/dead bacteria as a function of time after UV irradiation. *Bacillus* and *E. coli* bacteria were subjected to 5.5-mW/cm$^2$, 230~280-nm UV light for exposure times varying from 0.5 to 82 min. The bacteria absorption, fluorescence, and synchronous fluorescence spectra were recorded before and after each irradiation interval. The emission intensity in the 300–550-nm range was found to be the best for detecting the variation in the emission spectra before and after irradiation. For each PCA, we used the data obtained from at least two experiments, performed under identical conditions. The variation in emission spectra was attributed mainly to two principal components, deduced by PCA and depicted as scatter points in Fig. 5. The fluorescence spectra recorded at several time intervals for nonirradiated *Bacillus* (control) are shown in Fig. 5*A*, which indicates clearly that there is no significant difference between points. However, the emission spectra of the same bacteria show, in Fig. 5*B*, a clear separation between nonirradiated and irradiated bacteria as a function of UV irradiation time. The above experiment was repeated at least eight times to calibrate the process, which showed reasonable agreement with each other.

**Synchronous Fluorescence Spectra of *Bacillus* and *E. coli* Bacteria.** After each UV irradiation period, the bacteria were also plated and incubated for 24 h at 37 °C to determine the number of live bacteria in colony-forming units. Inactivation is defined in this study as the inability to reproduce (viability) after 48 h of incubation at 37 °C. The data presented in Fig. 6 show a sharp decrease in the number of live bacteria after 1 min or so of 5.5-mW/cm$^2$ UV irradiation. Essentially, the data suggest that most of the bacteria were inactive and the viable bacteria were reduced from $10^8$ to $10^2$ within 5 min of UV illumination. It is generally accepted that UV irradiation of bacteria affects mostly viability, because the bacterial damage caused by the UV is mainly in the form of nucleic acid dimerization: DNA dimerization (25). This is in contrast to reactions with chemical disinfectants, such as $O_3$, which lead to cell lysis. It is possible that DNA damage may be sufficient to prevent reproduction, yet allow them to repair sublethal damage and thus make it possible for them to perform some live bacteria functions.

The change in fluorescence band intensity of *Bacillus* bacterial strains, as a function of UV irradiation time, is shown in Fig. 7*A*. The change of the intensity maximum between 330 and 335 nm with UV illumination time is plotted in Fig. 7*B*. A close inspection of the fluorescence spectra reveals that the intensity of the 330~335-nm fluorescence band increased during the first

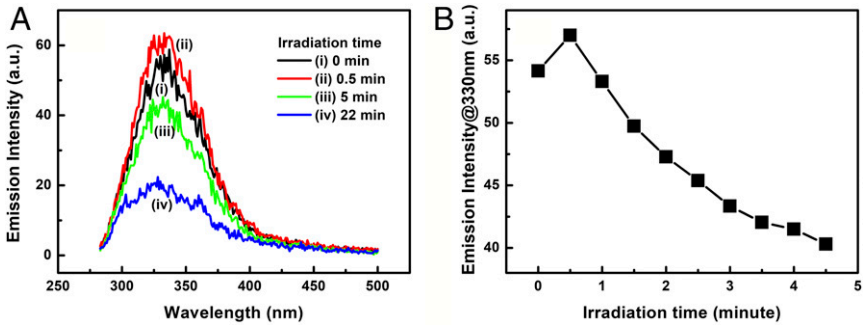


**Fig. 7.** (*A*) Fluorescence spectra of *Bacillus* irradiated with 5.5-W/cm$^2$, 230–280-nm UV light. Spectra (*i*), (*ii*), (*iii*), and (*iv*) were recorded after 0, 0.5, 5, and 22 min of UV irradiation, respectively. (*B*) Intensity change of the 330-nm fluorescence band maximum of *Bacillus* in saline irradiated with 5.5-mW/cm$^2$ as a function of irradiation time.

**Table 1. *Bacillus* bacteria cell viability lost as a function of irradiation time**

| Irradiation time, min | Alive (viable) | Dead (nonviable) |
|---|---|---|
| 0 | O O O O O O O | — |
| 5 | O O O O | X X X |
| 22 | O | X X X X X X |

Each O and X corresponds to log10 bacteria. Irradiation was performed with 5.5-mW/cm$^2$, 230~280-nm UV light.

minute of UV irradiation and then decreased continuously as a function of UV irradiation time. Similar results were also observed with *E. coli* bacteria. Because the fluorescence intensity is a measure of the concentration of the bacteria in the sample, a decrease in intensity designates a decrease in the number of bacteria per milliliter. The 330-nm peak displayed in the fluorescence spectra of *Bacillus* and *E. coli* is most probably due to tryptophan and therefore the initial increase and subsequent decrease in this fluorescence band intensity may correspond to an increase and subsequent decrease in tryptophan concentration. We performed similar experiments with Trp alone and mixtures of Trp and Tyr in water and saline solutions and did not observe any initial increase in the emission intensity, but only a continuous decrease of both the 330-nm intensity and the entire fluorescence spectrum as a function of irradiation time. We propose that some tryptophan, which was bonded to the bacteria membrane and therefore did not exhibit the same tryptophan emission maximum, was cleaved by the UV radiation, providing an additional amount of free tryptophan and thus the small initial increase in the 330-nm band intensity of *Bacillus* and *E. coli* spectra. We are performing additional experiments aimed at identifying the mechanism of the increase of the 330-nm bacterial fluorescence band during the first minute of UV irradiation. In addition, we are using Raman and coherent anti-Stokes Raman spectroscopy for the study of the Trp-membrane bond dissociation which may result in free Trp and thus help explain the observed increase in the 330-nm bacterial fluorescence band intensity maximum. Increasing the UV radiation time, or dose, results in the well-known degradation of Trp and consequently the decrease in the band intensity.

As noted above, plating data shown in Table 1 reveal that *Bacillus* viability is lost for 90% of the bacteria during the first 5 min of UV irradiation, which is similar to that found in *E. coli* under the same experimental condition. This is consistent with the bacterial membrane-Trp bond cleavage result, which generates some free Trp and forms a "hole" in the membrane that allows the UV radiation to penetrate through the bacteria wall, react with nucleic acid(s), and dimerize DNA. The measured inactivation response of both bacteria strains essentially suggests that only 100–500 cells per milliliter live bacteria remained, from the original $10^7$ cells per milliliter after about 10–20-min irradiation with 5.5-mW/cm$^2$ UV light. It has been proposed (26, 27) that a larger amount of respiratory bacteria survived after an equal irradiation dose. Microscopic examination of the bacteria samples we used indicated that before UV irradiation, the bacteria were single, or possibly in some cases paired; therefore, we consider the UV light interacts with nonaggregated bacteria. It has been reported that at higher UV doses a small fraction remains unaffected, such as the 100–500 viable bacteria found in our studies after 20 min of UV irradiation. A possible reason is the formation of dead bacteria aggregates which envelop live bacteria and shield them from the destructive effects of UV irradiation. Microscopic studies suggest that aggregation does develop after prolonged irradiation. It is interesting to note that the resistance to inactivation observed in aggregated bacteria, which is widely believed to be dimerization of cellular nucleic acid, DNA, is not transmitted to successive generations. Therefore, we consider aggregation as a bacterial defense mechanism against radiation damage and other forms of stress which may also result in aggregation (28, 29).

Owing to the fact that treatment with antibiotics is a preferable means for bacteria disinfection, we treated $10^8$ cells per milliliter *E. coli* with 100 μg/mL Ampicillin for 5 min, 22 min, 4 h, and 24 h. Plating and overnight incubating show that after 5 and 22 min of Ampicillin treatment, the bacteria population did not change; however, about $10^5$ cells per milliliter bacteria were killed after 4 h of treatment and all bacteria were killed after 24 h of treatment. Using the same synchronous fluorescence and PCA method described above, the separation of live and dead bacteria after each treatment period were clearly displayed on plot. We are performing experiments with Ampicillin and other antibiotics to establish the value of this method in determining the identity and ratio of live/dead bacteria in situ within minutes.

The handheld synchronous spectrometer may also record normal and synchronous fluorescence spectra of bacteria mixtures of different strains. The characteristic spectra of each strain may be distinguished by the synchronous fluorescence, and the live/dead bacteria ratio could be revealed by PCA. In addition, this device may also make possible the identification of the components such as tryptophan, tyrosine, and DNA of many strains of bacteria.

## Conclusion

The data presented in this paper show that it is possible to record in situ the normal and synchronous fluorescence spectra of bacteria and mixtures. Our data also show that by such techniques we may identify the components of bacteria and chemical mixtures and clearly display the fluorescence bands of the individual components. In addition, it is possible to distinguish between live and dead bacteria and determine the ratio of live/dead bacteria as a function of UV irradiation dose and antibiotic treatment that result in bacteria inactivation. It may even be possible to perform such assays directly on patient samples such as urine, cerebrospinal fluid, pleural fluid, or other body fluids either by adding antibiotics directly to these fluids and assessing the change in the ratio of live-to-dead bacteria or after the initiation of the treatment by determining the increasing proportion of dead bacteria.

**ACKNOWLEDGMENTS.** We thank Arjun Krishnamoorthi and Matthew Walck for valuable technical assistance. We are grateful for support of this research by The Welch Foundation Grant 1501928 and Texas A&M Engineering Experiment Station funds. J.C. acknowledges the support of the National Natural Science Foundation of China under Grants 61222509 and 11421064, and the Interdisciplinary Program of Shanghai Jiao Tong University under Project YG2015MS10.

1. McNamara L (2009) Health care-associated infection. *Am J Crit Care* 18:41.
2. Chittawatanarat K, Jaipakdee W, Chotirosniramit N, Chandacham K, Jirapongcharoenlap T (2014) Microbiology, resistance patterns, and risk factors of mortality in ventilator-associated bacterial pneumonia in a Northern Thai tertiary-care university based general surgical intensive care unit. *Infect Drug Resist* 7:203–210.
3. Hidron AI, et al.; National Healthcare Safety Network Team; Participating National Healthcare Safety Network Facilities (2008) NHSN annual update: Antimicrobial-resistant pathogens associated with healthcare-associated infections: Annual summary of data reported to the National Healthcare Safety Network at the Centers for Disease Control and Prevention, 2006-2007. *Infect Control Hosp Epidemiol* 29:996–1011.
4. Sievert DM, et al.; National Healthcare Safety Network (NHSN) Team and Participating NHSN Facilities (2013) Antimicrobial-resistant pathogens associated with healthcare-associated infections: Summary of data reported to the National Healthcare Safety Network at the Centers for Disease Control and Prevention, 2009-2010. *Infect Control Hosp Epidemiol* 34:1–14.
5. Tamma PD, et al. (2016) Comparing the outcomes of patients with carbapenemase-producing and non-carbapenemase-producing carbapenem-resistant Enterobacteriaceae bacteremia. *Clin Infect Dis* 64:257–264.
6. Handwerger S, et al. (1993) Nosocomial outbreak due to Enterococcus faecium highly resistant to vancomycin, penicillin, and gentamicin. *Clin Infect Dis* 16:750–755.

7. Lolans K, Thomas W, Munoz-Price LS, Quinn JP (2006) Multicity outbreak of carbapenem-resistant Acinetobacter baumannii isolates producing the carbapenemase OXA-40. *Antimicrob Agents Chemother* 50:2941–2945.
8. Manohar P, et al. (2017) The distribution of carbapenem- and colistin-resistance in Gram-negative bacteria from the Tamil Nadu region in India. *J Med Microbiol* 66: 874–883.
9. Bartlett JG, Gilbert DN, Spellberg B (2013) Seven ways to preserve the miracle of antibiotics. *Clin Infect Dis* 56:1445–1450.
10. Michael J, et al. (2017) Multicenter clinical and molecular epidemiological analysis of bacteremia due to carbapenem-resistant Enterobacteriaceae (CRE) in the CRE epicenter of the United States. *Antimicrob Agents Chemother* 61:e02349–16.
11. Ventola CL (2015) The antibiotic resistance crisis: Part 1: Causes and threats. *P&T* 40: 277–283.
12. Leblanc L, Dufour E (2002) Monitoring the identity of bacteria using their intrinsic fluorescence. *FEMS Microbiol Lett* 211:147–153.
13. Kumar A, et al. (2006) Duration of hypotension before initiation of effective antimicrobial therapy is the critical determinant of survival in human septic shock. *Crit Care Med* 34:1589–1596.
14. Kang C-I, et al. (2005) Bloodstream infections caused by antibiotic-resistant gram-negative bacilli: Risk factors for mortality and impact of inappropriate initial antimicrobial therapy on outcome. *Antimicrob Agents Chemother* 49:760–766.
15. Centres for Disease Control and Prevention (2013) Antibiotic resistance threats in the United States, 2013. Available at https://www.cdc.gov/drugresistance/pdf/ar-threats-2013-508.pdf. Accessed December 28, 2017.
16. Sohn M, Himmelsbach DS, Barton FE, 2nd, Fedorka-Cray PJ (2009) Fluorescence spectroscopy for rapid detection and classification of bacterial pathogens. *Appl Spectrosc* 63:1251–1255.
17. Ammor S, Yaakoubi K, Chevallier I, Dufour E (2004) Identification by fluorescence spectroscopy of lactic acid bacteria isolated from a small-scale facility producing traditional dry sausages. *J Microbiol Methods* 59:271–281.
18. Vo-Dinh T (1978) Multicomponent analysis by synchronous luminescence spectrometry. *Anal Chem* 50:396–401.
19. Bhatta H, Goldys EM, Learmonth RP (2006) Use of fluorescence spectroscopy to differentiate yeast and bacterial cells. *Appl Microbiol Biotechnol* 71:121–126.
20. Lloyd JBF (1971) Synchronized excitation of fluorescence emission spectra. *Nature* 231:64–65.
21. Runze Li, et al. (2017) Hand-held synchronous scan spectrometer for in situ and immediate detection of live/dead bacteria ratio. *Rev Sci Instrum* 88:114301.
22. Hoberman A, et al. (2003) Imaging studies after a first febrile urinary tract infection in young children. *N Engl J Med* 348:195–202.
23. Shaikh N, Morone NE, Bost JE, Farrell MH (2008) Prevalence of urinary tract infection in childhood: A meta-analysis. *Pediatr Infect Dis J* 27:302–308.
24. Blatchley ER, 3rd, Dumoutier N, Halaby TN, Levi Y, Laîné JM (2001) Bacterial responses to ultraviolet irradiation. *Water Sci Technol* 43:179–186.
25. Lyn DA, Chiu K, Blatchley ER, III (1999) Numerical modeling of flow and disinfection in UV disinfection channels. *J Environ Eng* 125:17–26.
26. Severin BF, Suidan MT, Engelbrecht RS (1983) Kinetic modeling of U.V. disinfection of water. *Water Res* 17:1669–1678.
27. Fletcher M, Marshall KC (1982) Are solid surfaces of ecological significance to aquatic bacteria? *Advances in Microbial Ecology* (Springer, New York), pp 199–236.
28. Bossier P, Verstraete W (1996) Triggers for microbial aggregation in activated sludge? *Appl Microbiol Biotechnol* 45:1–6.
29. Vo-Dinh T (1982) Synchronous luminescence spectroscopy: Methodology and applicability. *Appl Spectrosc* 36:576–581.